Volume 20
Number 9
September 1981

Inorganic Chemistry

Contribution from the Chemical Crystallography Laboratory, Oxford University, Oxford, OX1 3PD, England, the Department of Chemistry, University of Missouri—Rolla, Rolla, Missouri 65401, and the Nuclear Physics Division, Atomic Energy Research Establishment, Harwell, Didcot, OX11 ORA, England

Investigation of the Mixed-Metal Sulfide $(Mn,Fe)S_2$ by Analytical Electron Microscopy and Mössbauer Spectroscopy

ANTHONY K. CHEETHAM,*[1a] ALEXANDRA J. COLE,[1a] and GARY J. LONG*[1b]

Received November 10, 1980

The solid solutions of the $(Mn,Fe)S_2$ system have been prepared by a hydrothermal method. Microanalysis in a transmission electron microscope has indicated that the solubility of FeS_2 in MnS_2 is 6.0 (4) mol % and that the solubility of MnS_2 in FeS_2 is 3.9 (3) mol %. Mössbauer effect spectroscopy has shown that the manganese-rich solid solution contains high-spin divalent iron with a quadrupole interaction of 1.72 (2) mm/s and a chemical isomer shift of 0.96 (2) mm/s. The iron-rich phase contains only low-spin divalent iron with a quadrupole interaction of 0.63 (2) mm/s and an isomer shift of 0.42 (2) mm/s. The sulfur in the iron-rich material shows a tendency to oxidize to the sulfate ion upon standing in air for several days.

Introduction

The stoichiometric disulfides of manganese, iron, cobalt, and nickel accommodate the disulfide ion in the primitive cubic pyrites structure.[2] They occur naturally as mineral deposits and, with the exception of MnS_2 which must be made hydrothermally,[3] they may be obtained by the direct interaction of the elements. MnS_2 decomposes to α-MnS above 250 °C,[4] the remaining disulfides are thermally stable. Whereas FeS_2 and CoS_2 contain low-spin divalent iron and cobalt, the divalent manganese in MnS_2 adopts the high-spin electronic configuration.

The continuous series of solid solutions at elevated temperatures in the $(Fe,Co)S_2$ and $(Co,Ni)S_2$ systems[5] and the limited mutual solubility of FeS_2 and NiS_2[6] have been extensively invesitgated. In contrast there have been relatively few detailed studies of the phase diagrams of MnS_2 with the other disulfides. At high temperatures and pressures, Bither et al.[7] have prepared the continuous series of solid solutions of $(Mn,Zn)S_2$, $(Mn,Cu)S_2$, and $(Mn,Cd)S_2$. Bargeron et al.[8] have studied the Mössbauer spectrum of MnS_2 doped with iron-57. They report that the divalent iron is high spin at atmospheric pressure and undergoes a reversible high-spin to low-spin electronic transition between 40 and 120 kbar. Adachi et al.[9] report the preparation of FeS_2 doped with up to 5.6 mol % of MnS_2, but their magnetic measurements, which suggest the presence of divalent high-spin manganese, reveal a Curie–Weiss constant which surprisingly decreases with increasing manganese content.

We have investigated the $(Mn,Fe)S_2$ system by microanalysis in an electron microscope in order to determine the phase equilibria. The results reported herein provide an excellent illustration of the efficacy of the microanalytical technique for studying phase diagrams. We have also studied the nature of the electronic spin state of the iron in these systems by Mössbauer spectroscopy.

Experimental Section

The method of hydrothermal synthesis of MnS_2, first described by Blitz and Weichmann[3] and more recently by Auroux et al.[4] and Avinon and dePasquali,[10] was adapted to prepare samples of $Mn_xFe_{1-x}S_2$. The starting materials were accurately determined mixtures of AnalaR reagent $FeSO_4 \cdot 7H_2O$ and $MnSO_4 \cdot H_2O$ and potassium polysulfide solution. The products were collected, purified, and dried as described by the earlier workers.[3,4,10]

A JEOL 100CX Temscan analytical electron microscope was used for accurate elemental analysis. The X-ray emission from a microvolume of sample was detected by a lithium-drifted silicon detector. The finely ground sample was dispersed on a copper-mesh grid coated with a holey carbon film. The sample grid was tilted at 40°, and X-ray counts were collected for 100 s of live time at an accelerating voltage of 100 kV. Small individual crystallites of the sample were chosen for quantitative analysis by the "ratio method" which applies to thin crystals where absorption and fluorescence effects can be considered negligible.[11] The ratio of the concentrations of two elements, A and B, is proportional to the ratio of the intensities of two X-ray lines, characteristic of those elements, i.e., $C_A/C_B = kI_A/I_B$. The value of the constant, k, for each pair of elements was obtained from synthetic and natural FeS_2 and MnS_2 standards. Analysis on many different crystals of FeS_2 on three separate occasions gave k values for Fe/S

(1) (a) Oxford University. (b) University of Missouri—Rolla and the Atomic Energy Research Establishment, Harwell. (Address correspondence to A.K.C. at the University of Oxford and to G.J.L. at the University of Missouri.)
(2) Elliott, N. *J. Chem. Phys.* **1960**, *33*, 903.
(3) Blitz, W.; Weichman, F. *Z. Anorg. Allg. Chem.* **1936**, *229*, 268.
(4) Auroux, A.; Bonnetot, B.; Bonsquet, J. *Bull. Soc. Chim. Fr.* **1971**, *11*, 3904.
(5) Bouchard, R. J. *Mater. Res. Bull.* **1968**, *3*, 563. Nishihara, Y.; Ogawa, S. *Phys. Rev. B: Condens. Matter* **1980**, *22*, 5453.
(6) Clark, L. A.; Kullerud, G. *Econ. Geol.* **1963**, *58*, 853.
(7) Bither, T. A.; Donohue, P. C.; Cloud, W. H.; Bierstedt, P. E.; Young, H. S. *J. Solid State Chem.* **1970**, *1*, 526.
(8) Bargeron, C. B.; Avinor, M.; Drickamer, H. G. *Inorg. Chem.* **1971**, *10*, 1338.
(9) Adachi, K.; Ueno, T.; Sawamoto, H. *J. Phys. Soc., Jpn.* **1976**, *41*, 1069.
(10) Avinon, M.; dePasquali, G. *J. Inorg. Nucl. Chem.* **1970**, *32*, 3403.
(11) Cliff, G.; Lorimer, G., W. *J. Microsc. (Oxford)* **1975**, *103*, 203.

0020-1669/81/1320-2747$01.25/0

Table I. Results from Several Hydrothermal Preparations

major component	Mn:Fe[a]	prep temp, °C	physical properties	phases[b]
$Mn_{0.04}Fe_{0.96}S_2$	5:95	300	black, microcrystalline	$Mn_{0.038(4)}Fe_{0.962(4)}S_{2.02(5)}$, MnS_2
$Mn_{0.04}Fe_{0.96}S_2$	10:90	300	black, microcrystalline	$Mn_{0.041(3)}Fe_{0.959(3)}S_{2.04(7)}$, MnS_2
$Mn_{0.94}Fe_{0.06}S_2$	95:5	240	dark red, highly crystalline	$Mn_{0.940(4)}Fe_{0.060(4)}S_{1.98(8)}$, $Mn_{0.040(5)}Fe_{0.960(5)}S_{2.09(10)}$, MnS_2

[a] Preparative ratio. [b] Characterized by X-ray microanalysis.

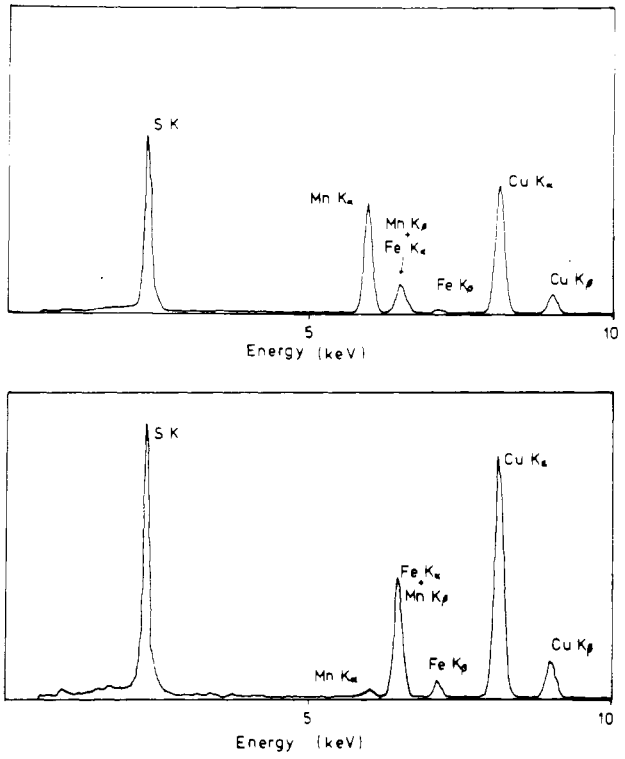

Figure 1. X-ray emission spectra of the limiting solid solutions in the $(Mn,Fe)S_2$ mixed-metal system. The copper peaks arise from the copper sample grid.

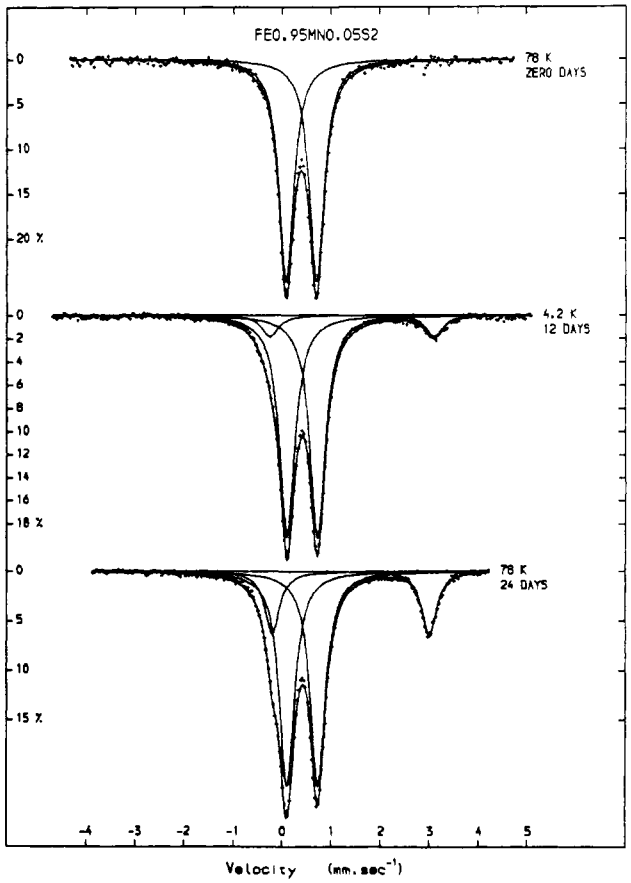

Figure 2. Mössbauer-effect spectra of $Mn_{0.04}Fe_{0.96}S_2$ obtained after 0, 12, and 24 days. The minor component present at 12 and 24 days corresponds to an iron sulfate impurity.

of 0.79, 0.77, and 0.78 with a standard deviation of 0.01. For MnS_2, k values of 0.75 and 0.73, with a standard deviation 0.01, were obtained. The stoichiometries of the $(Mn,Fe)S_2$ products were calculated with these constants. It was necessary to make a correction for the overlap of the Fe Kα and Mn Kβ X-ray lines. The intensity of the Mn Kβ peak was found, from the standard MnS_2, to be 13.0 (1)% of the Mn Kα peak, in excellent agreement with another recent determination.[12] The Fe Kα intensity was found by subtraction.

Mössbauer effect absorbers were prepared from fine powders, which were mixed with vaseline to provide a random polycrystalline sample with a uniform thickness of approximately 7 mg/cm^2 of natural abundance iron. The Mössbauer spectra were obtained on a Harwell constant-acceleration spectrometer which utilized a room-temperature rhodium matrix source and was calibrated with natural α-iron foil at room temperature. The 4.2 K spectra were obtained in a cryostat in which the sample was placed directly in liquid helium. The Mössbauer spectra were evaluated by using least-squares minimization programs. In all cases, the two component lines of a quadrupole split doublet were constrained to have the same areas and line widths. In most instances, the removal of these constraints resulted in only minor changes in the Mössbauer spectral parameters and only a marginal improvement in χ^2. More details of the fitting procedures used may be found elsewhere.[13] The Mössbauer effect parameters reported herein have error limits of approximately ±0.02 mm/s.

Results and Discussion

Samples were prepared with various manganese-to-iron ratios and at temperatures between 200 and 300 °C. The hydrothermal reaction time was approximately 48 h in all cases. The products were very fine powders, varying in color from black to dark red. Samples prepared at low temperature were virtually amorphous as indicated by their X-ray powder diffraction patterns. However, X-ray powder diffraction patterns of the high-temperature preparations all contained weak but distinct MnS_2 lines, irrespective of the initial composition. In these samples, a few crystals of pure MnS_2 were also found by microanalysis, suggesting that MnS_2 may be a kinetically controlled product in this hydrothermal reaction. The X-ray powder patterns of samples rich in iron contained diffuse X-ray lines close to those expected for FeS_2.

The results from three typical preparations are presented in Table I. The products obtained in the reactions with a low manganese-to-iron preparative ratio exhibit rather poorly defined X-ray powder diffraction patterns. However, the crystallites exhibited a well-defined morphology in the electron microscope. In contrast, the preparation with the high manganese content was highly crystalline. The X-ray microanalysis

(12) Heinrich, K. F. J.; Fiori, C. E.; Myklebust, R. L. *J. Appl. Phys.* **1979**, *50*, 5589.
(13) Long, G. J.; Longworth, G.; Day. P.; Beveridge, D. *Inorg. Chem.* **1980**, *19*, 821.

Table II. Mössbauer Effect Spectral Parameters[a]

compd	age, days	spin state	T, K	ΔE_Q	δ	$\Gamma_{1/2}$	% area
FeS_2 (natural)		low spin	294	0.61	0.31	0.29	100
		low spin	78	0.62	0.40	0.29	100
$Mn_{0.04}Fe_{0.96}S_2$	0	low spin	78	0.63	0.40	0.36	100
	12	low spin	4.2	0.62	0.42	0.38	91
		high spin[b]		3.35	1.44	0.41	9
	24	low spin	78	0.63	0.42	0.37	78
		high spin[b]		3.20	1.40	0.36	22
	115	low spin	294	0.61	0.32	0.34	80
		high spin[b]		2.74	1.25	0.29	10
				3.19	1.23	0.41	10
	115	low spin	78	0.62	0.42	0.36	73
		high spin[b]		3.19	1.40	0.39	27
	270	low spin	78	0.61	0.42	0.36	73
		high spin[b]		3.18	1.38	0.38	27
$Mn_{0.04}Fe_{0.96}S_2$[c]		low spin	78	0.60	0.44	0.33	34
$Mn_{0.94}Fe_{0.06}S_2$[c]		high spin		1.72	0.96	0.33	66
$FeSO_4 \cdot 7H_2O$		high spin	298	3.18	1.23	0.32	100
			78	3.35	1.35	0.37	100
$Mn(^{57}Fe)S_2$[d]		low spin	room temp	0.60	0.35		
		high spin		1.50	0.84		

[a] All data in mm/s relative to natural α-iron foil. [b] Resulting from $FeSO_4$ species. [c] Biphasic material. [d] Data from ref 8.

results given in Table I are the mean values obtained from measurements on many crystals. These results indicate that the solubility of MnS_2 in FeS_2 is 3.9 ± 0.3 mol % and that of FeS_2 in MnS_2 is 6.0 ± 0.4 mol %. The X-ray emission spectra for the two limiting solid solutions are given in Figure 1.

Mössbauer effect spectra were measured for the second and third preparations listed in Table I as well as for freshly ground single crystals of natural pyrite, FeS_2, and $FeSO_4 \cdot 7H_2O$. The resulting spectral parameters are presented in Table II. The Mössbauer spectrum of a fresh sample of $Mn_{0.04}Fe_{0.96}S_2$, illustrated at the top of Figure 2, exhibits a quadrupole split doublet which is characteristic of low-spin iron(II). The isomer shift, δ, and quadrupole splitting, ΔE_Q, are in close agreement with the values obtained for a freshly ground sample of natural FeS_2 (see Table II) and with values reported earlier.[14,15] The only real difference is in the absorption line width, $\Gamma_{1/2}$. The significantly higher value of 0.36 mm/s for $Mn_{0.04}Fe_{0.96}S_2$ as compared with 0.29 mm/s for natural FeS_2 may be attributed partly to the presence of the manganese and partly to the presence of a high level of defects and a large surface area in $Mn_{0.04}Fe_{0.96}S_2$ prepared by hydrothermal techniques.

A reexamination of this sample after 12, 24, 115, and 270 days revealed the partial decomposition of this material to a phase containing high-spin iron(II) with a quadrupole splitting of 3.2 mm/s and an isomer shift of 1.4 mm/s at 78 K (see Figure 2 and Table II). The appearance of this decomposition product is most rapid immediately after preparation. Smaller increases in the amount of the decomposition product are apparent at 115 and 270 days. The 78 K spectra obtained at 115 and 270 days are essentially identical to that shown for 24 days in Figure 2. The presence of this high-spin component suggests that our microcrystalline FeS_2-rich product is undergoing aerial oxidation to some form of $FeSO_4$ over a period of time. A subsequent reexamination of aged iron-rich samples in the electron microscope also revealed a substantial number of crystals with a metal-to-sulfur ratio close to unity. These older samples also gave a positive test for the sulfate ion with barium chloride. The tendency to decompose appeared to be most pronounced with amorphous samples prepared at lower temperatures.

The exact nature of this impurity is not completely clear at this point. It may represent a highly dispersed form of α-$FeSO_4$ which is reported[16,17] to have Mössbauer parameters very similar to those observed for the impurity. However, this compound is known[17] to order as a uniaxial antiferromagnet at 24 K. Hence, if α-$FeSO_4$ is the oxidation product, it must be present in a highly dispersed superparamagnetic form. Alternatively, and probably more likely, the impurity is similar to $FeSO_4 \cdot 7H_2O$, which is found to have a quadrupole splitting of 3.18 mm/s and an isomer shift of 1.23 mm/s at 293 K, values in good agreement with earlier work.[18] It does not order at low temperatures. It should be noted that the impurity has a rather large line width and at 294 K is best fitted with two partially resolved components with essentially the same isomer shift but different quadrupole splittings. This probably indicates that we have $FeSO_4$ present in a variety of different hydration states.

Scheme I

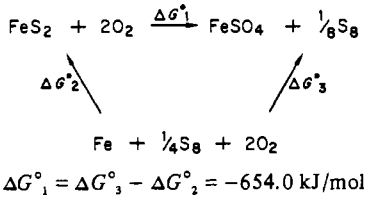

$\Delta G^\circ_1 = \Delta G^\circ_3 - \Delta G^\circ_2 = -654.0$ kJ/mol

The aerial oxidation of FeS_2 to $FeSO_4$ at 298 K is thermodynamically favorable (see Scheme I) because the standard Gibbs free energies of formation are −166.9 kJ/mol for FeS_2 and −820.9 kJ/mol for $FeSO_4$.[19] The oxidation of the FeS_2-rich solid solution is presumably kinetically feasible because of the poor crystallinity of this material.

The Mössbauer spectrum of the material resulting from the manganese-rich preparation is shown in Figure 3, and the resulting parameters are given in Table II. In agreement with the microanalytical results, the spectrum indicates the presence of two iron-containing phases. If we assume that the iron in the two phases has the same recoil free fraction, then it is apparent that the material contains 97% of $Mn_{0.94}Fe_{0.06}S_2$—corresponding to the major component in the spectrum—and 3% of $Mn_{0.04}Fe_{0.96}S_2$. This latter component has Mössbauer spectral parameters which are essentially the same as those

(14) Temperley, A.; Lefevre, H. *J. Phys. Chem. Solids* **1966**, *27*, 85.
(15) Nishihara, Y.; Ogawa, S. *J. Chem. Phys.* **1979**, *71*, 3796.
(16) Ono, K.; Ito, I. *J. Phys. Soc. Jpn.* **1964**, *19*, 899.
(17) Wehner, H. L.; Spiering, H.; Ritter, G. *Solid State Commun.* **1976**, *20*, 831.
(18) Meisel, W.; Kreysa, G. *Z. Anorg. Allg. Chem.* **1973**, *395*, 31.
(19) *NBS Tech. Note (U. S.)* **1965**, *No.* 270/1.

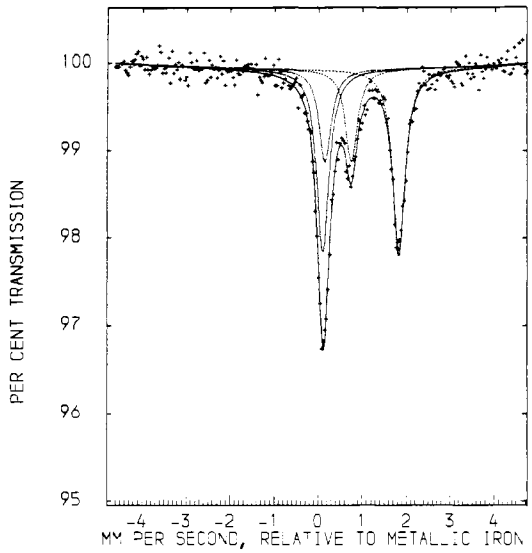

Figure 3. The 78 K Mössbauer-effect spectrum of a biphasic mixture containing the two limiting solid solutions. The major component is high-spin $Mn_{0.94}Fe_{0.06}S_2$. The minor component is low-spin $Mn_{0.04}Fe_{0.96}S_2$.

of the low-spin iron in $Mn_{0.04}Fe_{0.96}S_2$ prepared directly. The spectrum of this material shows no indication of the presence of an iron-containing sulfate impurity. The Mössbauer parameters for the iron site in $Mn_{0.94}Fe_{0.06}S_2$ indicate that in the MnS_2 lattice the iron adopts the high-spin, $^5T_{2g}$, electronic configuration. Our results are similar to those of Bargeron et al.,[8] who found that iron-57 as a dilute substitutional impurity in MnS_2 was high spin at pressures below ca. 40 kbar. Above this pressure, the iron is slowly converted with increasing pressure to the low-spin state.[8] In agreement with these authors,[8] we believe that the change in the electronic spin state of iron in going from FeS_2 to $Mn_{0.94}Fe_{0.06}S_2$ results from the reduction in the ligand field potential as the lattice parameter increases. The lattice parameter, a, for FeS_2 is 5.504 Å[8] whereas for MnS_2 it is 6.102 Å.[20] The proportions of the two iron-containing phases determined from the Mössbauer spectrum are in agreement with the starting composition and the observed phase limits, when the kinetic formation of pure MnS_2 is taken into consideration.

Our result for the solubility of MnS_2 in FeS_2 does not agree with the value of 5.6 mol % reported by Adachi et al.[9] Furthermore, our confirmation that $Mn_{0.04}Fe_{0.96}S_2$ contains low-spin iron(II) suggests that FeS_2 will be unable to accommodate the much larger high-spin manganese(II) ion and that the manganese(II) is present in the low-spin configuration. We have been unable to reproduce the preparation by using the method of Adachi et al.[9], and it is possible that they synthesized FeS_2 plus small quantities of (Mn,Fe)S. This interpretation would also account for their observation that the lattice parameter of their FeS_2 solid solution does not vary with manganese content. The greater solubility observed for iron in MnS_2 than for manganese in FeS_2 is consistent with the relative ease with which divalent iron can adopt either the high-spin or the low-spin electronic configuration.

Acknowledgment. It is a pleasure to acknowledge the assistance and the helpful discussions that we have had with Drs. G. Longworth and T. E. Cranshaw and Mr. B. Laundy during the course of this work. We also wish to thank the Science Research Council for a grant (GR/A/3320) toward the purchase of the electron microscope.

Registry No. FeS_2, 12068-85-8; MnS_2, 12125-23-4.

(20) Westrum, E. F.; Gronvold, F. *J. Chem. Phys.* **1970**, *52*, 3820.

Contribution from the Fachbereich Chemie und Sonderforschungsbereich 127 "Kristallstruktur und chemische Bindung" der Philipps-Universität Marburg, 3550 Marburg, GFR

Local and Cooperative Jahn-Teller Interactions of Copper(2+) in Host Lattices with Tetragonally Compressed Octahedra. Spectroscopic and Structural Investigation of the Mixed Crystals $K(Rb)_2Zn_{1-x}Cu_xF_4$

D. REINEN* and S. KRAUSE

Received September 29, 1980

The **g** tensor of the mixed crystals $K(Rb)_2Zn_{1-x}Cu_xF_4$ at high x values is exchange narrowed, corresponding to an antiferrodistortive order of elongated CuF_6 octahedra, with a distinct orthorhombic distortion component superimposed. At low x values the g parameters are in agreement with compressed octahedra in time average, with appreciable admixtures of $d_{x^2-y^2}$ into the d_{z^2} ground state, however. A model accounting for the change of g with x is proposed, which is based on the strain effect of the compressed ZnF_6 host lattice sites. The single-crystal and powder EPR data are supplemented by ligand field spectroscopic and structural information. In addition refined Cu-F bond lengths for K_2CuF_4 are given as the result of a neutron diffraction powder analysis. A set of approximate Jahn-Teller parameters (radial and angular distortion parameters ρ and φ, linear and nonlinear vibronic coupling constants V and V_3) for the mixed crystals with different Cu^{2+} concentrations could be evaluated, which is consistent with the available experimental information also for other copper(2+) fluoride compounds.

Introduction

Cu^{2+} ions in octahedral coordination undergo strong Jahn-Teller distortions, which correspond to a tetragonal elongation with frequently an orthorhombic symmetry component superimposed. This statement is correct only, however, if the host lattice sites are regularly octahedral and if the ligands are equal.[1] Cu^{2+} systems of this kind represent cases of strong linear Jahn-Teller coupling and the matrix[2]

$$\begin{pmatrix} {}^1/_2M\omega^2\rho^2 - V\rho\cos\varphi - V_3\rho^3\cos 3\varphi & V\rho\sin\varphi \\ V\rho\sin\varphi & {}^1/_2M\omega^2\rho^2 + V\rho\cos\varphi - V_3\rho^3\cos 3\varphi \end{pmatrix}$$

describes the energy changes occurring, if the electronic ^2E_g

0020-1669/81/1320-2750$01.25/0